International Journal of Nanomedicine

Dovepress
open access to scientific and medical research

Open Access Full Text Article

ORIGINAL RESEARCH

Pluronic F-127 Hydrogel Loaded with Human Adipose-Derived Stem Cell-Derived Exosomes Improve Fat Graft Survival via HIF-1α-Mediated Enhancement of Angiogenesis

Fangfang Yang[1,*], Zihao Li[2,*], Zhongming Cai[1], Yucang He[1], Chen Ke[1], Jingping Wang[1], Ming Lin[3], Liqun Li[1]

[1]Department of Plastic Surgery, The First Affiliated Hospital of Wenzhou Medical University, Wenzhou, Zhejiang, People's Republic of China; [2]Department of Wenzhou Medical University, Wenzhou, Zhejiang, People's Republic of China; [3]Department of Obstetrics and Gynecology, Second Affiliated Hospital and Yuying Children's Hospital of Wenzhou Medical University, Wenzhou, Zhejiang, People's Republic of China

*These authors contributed equally to this work

Correspondence: Liqun Li, Department of Plastic Surgery, The First Affiliated Hospital of Wenzhou Medical University, Wenzhou, Zhejiang, 325000, People's Republic of China, Tel +86 13706664412, Email wzliliqun@163.com

Purpose: Autologous fat grafting is playing an increasingly important role in plastic surgery. However, high absorption and low survival of autologous fat grafts limit their clinical application. This study aimed to investigate whether human adipose-derived stem cell-derived exosomes (hASC-Exos) encapsulated in a PF-127 hydrogel can improve the survival of autologous fat grafts and to elucidate the underlying mechanisms.

Patients and Methods: Exosomes were isolated from hASCs and identified using transmission electron microscopy, nanoparticle tracking analysis and Western blotting. We performed functional assays in vitro to assess the effect of hASC-Exos on proliferation, migration, and tube formation as well as their regulatory role in the HIF-1α/VEGF signaling pathway. hASC-Exos encapsulated in the PF-127 hydrogel were used as an in vivo autologous fat graft model. The effects of the PF-127 hydrogel/hASC-Exos and the role of the HIF-1α/VEGF signaling pathway in promoting angiogenesis in an autologous fat grafting model were assessed.

Results: hASC-Exos were taken up by human umbilical vein endothelial cells and enhanced their proliferation, migration, and tubule formation in vitro. The effects of hASC-Exos on promoting angiogenesis were mediated by the HIF-1α/VEGF signaling pathway. Moreover, we fabricated a PF-127 hydrogel for the sustained release of hASC-Exos, and in vivo results showed that hASC-Exos encapsulated in PF-127 hydrogel improved the survival of autologous fat grafts.

Conclusion: Our findings indicated that hASC-Exos encapsulated in PF-127 hydrogel serve as a key regulator of angiogenesis by activating the HIF-1α/VEGF signaling pathway and provide a promising strategy for autologous fat grafting treatment.

Keywords: autologous fat grafting, human adipose-derived stem cell, exosome, hydrogel, HIF-1α/VEGF signaling pathway, angiogenesis

Introduction

Autologous fat grafting has recently played an increasingly important role in plastic and aesthetic surgeries. It has been widely used in tissue repair and reconstruction, facial fat filling, breast reconstruction, and other related procedures, with significant advantages such as convenient access, good biocompatibility, and effectiveness.[1] However, the high absorption and low survival rates of autologous fat grafts limit their use and promotion of autologous fat. Therefore, improving the survival rate of autologous fat grafts is a critical issue that needs to be addressed. Previous studies have indicated that revascularization after transplantation is essential for the survival of the transplanted fat.[2–4] The newly formed

Received: 7 September 2023
Accepted: 9 November 2023
Published: 16 November 2023

Graphical Abstract

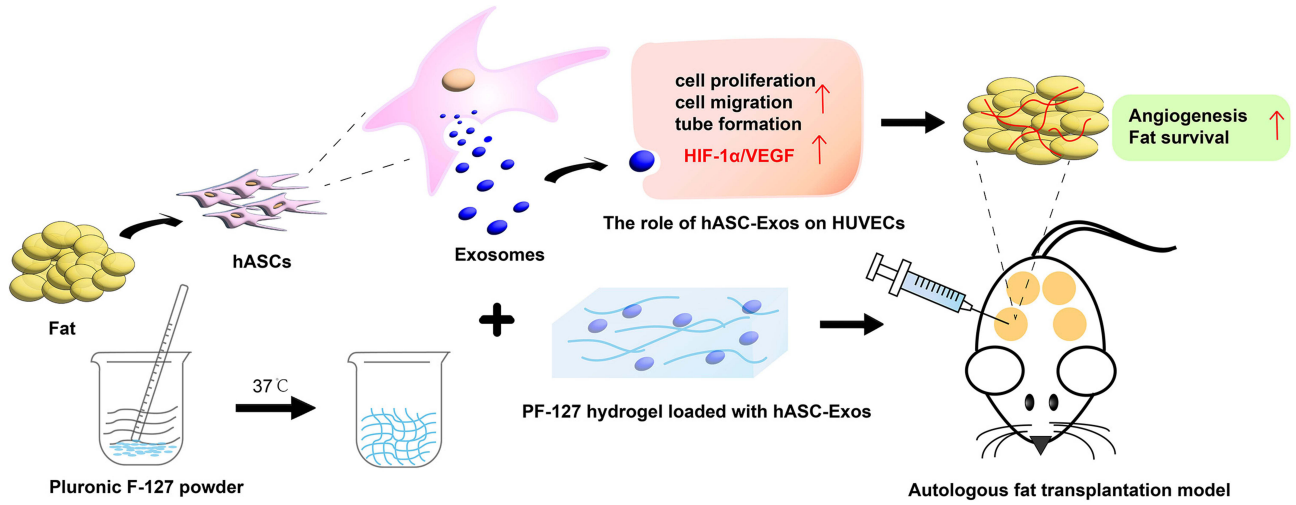

vasculature can provide oxygen and nutrition to the transplanted tissue.[5] Therefore, we consider promoting angiogenesis to be a key factor in improving the survival of autologous fat grafts.

Mesenchymal stem cells (MSCs) are appropriate for use in potential applications owing to their pluripotency and ease of harvesting.[6] They have rapidly become favored tools in regenerative medicine. Furthermore, a large number of studies have highlighted that stem cell research has enabled stem cell-based treatments, such as those based on umbilical cord-derived stem cells[7] and adipose-derived stem cells (ASCs),[8] to serve as promising alternatives for angiogenesis. Compared with other stem cells, ASCs possess desirable advantages such as abundant tissue sources, good amplification ability, and high yield.[9] ASCs appear to be a better choice for stem cell therapy in autologous fat transplantation. However, therapies involving stem cells still face potential dangers with regard to changes in differentiation ability,[10] embolism potential,[11] and immune rejection, which impose significant limitations on their clinical applications.[12]

Emerging evidence suggests that stem cell-derived exosomes are novel tools for tissue regeneration.[13,14] Exosomes (a type of small extracellular vesicle [sEVs] with a diameter of 30–150 nm) are rich in proteins, miRNAs, and lipids. Exosomes also play an important regulatory role in intercellular communication and biological processes.[15,16] Furthermore, recent studies have reported that exosomes generated from stem cells perform equally or better than MSCs.[10,11,13] Moreover, exosomes can provide cell-free therapy with various advantages, such as no risk of ectopic tissue formation, lower immunogenicity, and greater stability and storability.[17] Therefore, exosome-based therapies have emerged as one of the most promising strategies in regenerative medicine.[18] However, there are challenges in the application of exosomes because they are quickly eliminated by blood circulation or lymphatic transportation,[19] and direct local repeated injections can cause additional pain to patients. Thus, construction of a sustained-release platform for exosomes has emerged as the focus of exosome-based therapies.

Injectable thermosensitive hydrogels are promising carriers for exosomes.[20] Exosomes loaded within hydrogels can be used to control their release for longer durations and improve their therapeutic effects and efficiencies. Although several studies have shown the beneficial effects of exosome-loaded hydrogels in regenerative medicine, such as wound healing and bone repair,[21,22] whether Human adipose-derived stem cell (hASCs)-derived exosomes (hASC-Exos) combined with Pluronic F-127 hydrogel (PF-127, also known as Poloxamer 407) can improve the survival of autologous fat transplantation is unknown. PF-127 hydrogel, approved by the FDA, exhibited good temperature sensitivity, injectability, degradability and favorable biocompatibility.[23,24] In a previous study, we found that PF-127 possessed a highly porous structure that could prolong drug retention in vivo, thereby alleviating the symptoms of T2DM.[25] Furthermore, umbilical cord-derived stem cell-derived exosomes combined with a PF-127 hydrogel can promote skin regeneration.[23]

Based on these results, we hypothesized that the combined application of PF-127 hydrogel and hASC-Exos might improve the survival of autologous fat grafts.

In this study, we established an autologous fat transplantation mouse model to investigate the role of PF-127 hydrogel loaded with hASC-Exos in improving fat grafts survival. Moreover, the molecular mechanisms underlying the promotion of angiogenesis via HIF-1α/VEGF signaling pathway were further assessed. Our findings provide a promising approach for enhancing the therapeutic benefits of hASC-Exos and improving the survival rate of autologous fat grafts.

Materials and Methods

Cell Isolation, Identification, and Culture

This study was conducted in accordance with the guidelines approved by the Ethics Committee of the First Affiliated Hospital of Wenzhou Medical University (KY2023-015) and the Declaration of Helsinki. Adipose tissue was obtained from healthy young women who provided informed consent and underwent abdominal liposuction at the First Affiliated Hospital of Wenzhou Medical University. hASCs were isolated and confirmed as previously described with some modifications.[6,17,26,27] Briefly, the fat tissue was digested with 0.1% (w/v) type I collagenase (Sigma-Aldrich, St Louis, MO, USA) at 37°C for 50 min and digestion was terminated with the same volume of complete medium (OriCell, Guangzhou, China) containing 10% fetal bovine serum and 1% penicillin/streptomycin (Beyotime, Shanghai, China). Next, the digested hASCs were filtered, centrifuged, and resuspended in the complete culture medium as described above, and seeded at 37°C in a humidified 5% CO_2 atmosphere. The medium was replaced every other day, and cells from passages 3 to 6 were used for subsequent experiments.

Adipogenesis, osteogenesis, and chondrogenesis assays were performed using a specific differentiation medium (OriCell, Guangzhou, China) to characterize the multilineage differentiation potential of hASCs according to the manufacturer's protocol. hASCs were identified using flow cytometry. Briefly, cells at passage 3 were harvested and 1×10^5 cells were stained with specific fluorescent surface antibodies, including PE-conjugated anti-human CD29, CD31, CD44, CD45, CD90, and isotype IgG (all from BD Biosciences, San Jose, CA, USA).

Human umbilical vein endothelial cells (HUVECs) were obtained from Sigma-Aldrich and maintained in endothelial cell medium (ScienCell, San Diego, California, USA) containing 5% fetal bovine serum, 1% endothelial cell growth supplement and 1% penicillin/streptomycin (Beyotime, Shanghai, China) at 37°C in a humidified 5% CO_2 atmosphere.

Production, Isolation, and Characterization of hASC-Exos

hASC-Exos were isolated via ultracentrifugation according to a published protocol, with a few modifications.[28] Briefly, hASCs from passages 3 to 6 were cultured in exosome-free complete medium (OriCell, Guangzhou, China) and after culturing for 48 h, the cell-conditioned medium was harvested and centrifuged at 300 × g for 10 min, 2000 × g for 10 min, and 10,000 × g for 30 min at 4°C to remove the dead cells, cellular debris, and some large vesicles. Then, the supernatants were further filtered and transferred to new ultracentrifuge tubes and ultracentrifuged at 120,000 × g twice for 70 min at 4°C to obtain exosome pellets. Finally, the pellets were resuspended in 200 μL of cold phosphate-buffered saline (PBS) and stored at −80 °C for subsequent experiments.

The morphology of hASC-Exos was imaged using transmission electron microscopy (TEM) (JEOL, Tokyo, Japan), and the particle size distribution was estimated using nanoparticle tracking analysis (NTA) (Malvern Instruments, Malvern, UK). Exosome protein concentrations were determined using a bicinchoninic acid (BCA) Protein Assay Kit (Beyotime, Shanghai, China) and Western blotting was performed to examine the characteristic markers of exosomes, including CD9, CD63, TSG10, and calnexin.

hASC-Exo Labeling and Internalization Assays

To trace exosome internalization, hASC-Exos were labeled with 1,1′-dioctadecyl-3,3,3′,3′-tetramethylindocarbocyanine perchlorate (Dil, Beyotime, Shanghai, China) according to the manufacturer's instructions. Briefly, purified exosomes were incubated in 10 μM Dil solution and the labeled exosomes were obtained after ultracentrifugation at 120,000 × g for 70 min to remove excess dye. Subsequently, HUVECs were co-cultured with Dil-labeled exosomes for 24 h. Nuclei were

stained with 4′,6-diamidino-2-phenylindole (DAPI; Sigma-Aldrich, St Louis, MO, USA). Exosome uptake was visualized under a fluorescence microscope (Olympus, Tokyo, Japan).

Cell Proliferation Assay

The proliferation of HUVECs in response to exosomes was evaluated using the Cell Counting Kit-8 assay (CCK-8; Dojindo, Kumamoto, Japan) according to the manufacturer's protocol. Briefly, HUVECs were carefully seeded into 96-well culture plates and treated with 50 μg/mL hASC-Exos or same volume of PBS. After co-culturing for 1, 3, and 5 days, 10% CCK-8 solution was added to each well and incubated for 3 h at 37 °C. The proliferation rates were determined by measuring the optical density at 450 nm using a microplate reader (BioTek, Winooski, VT, USA).

Migration Assay

The effect of hASC-Exos on HUVEC migration was assessed using scratch and transwell assays. First, the scratch assay was performed in a 6-well plate. When the cellular confluence reached approximately 100%, a scratch wound was made using a sterile 200 μL pipette tip, Next, the cells were left to grow for an additional 0, 12, and 24 h at 37 °C in the presence of 50 μg/mL hASC-Exos or PBS. Finally, an inverted microscope was used to record the images, and the migration distance was quantified using ImageJ software.

During the transwell assay, 1×10^5 cells treated with 50 μg/mL hASC-Exos or PBS in serum-free medium were seeded into the upper chamber of a transwell plate and allowed to migrate for 24 h. Subsequently, migrated cells were photographed under an optical microscope and quantified using ImageJ software.

Tube Formation Assay

To investigate the pro-angiogenic effect of hASC-Exos on HUVECs in vitro, a tube formation experiment was performed as previously described.[29] Briefly, 50 μL of cold Matrigel (BD Biosciences, San Jose, CA, USA) was placed onto a 96-well plate and allowed to gel for 30 min. Then, HUVECs (2×10^4 cells/well) were seeded on the Matrigel-covered well and treated with FBS-free media in the presence of hASC-Exo (50 μg/mL) or PBS as the control. After incubation for 6 h, endothelial network development was observed under a bright-field microscope (Olympus, Tokyo, Japan). The number of total meshes, branch points, and tubule lengths in three randomly chosen fields in each well were quantified using ImageJ software.

Western Blot Analysis

Western blotting was performed according to standard protocols. Briefly, total proteins from exosomes/cells were harvested using radioimmunoprecipitation assay (RIPA) lysis buffer (Solarbio, Shanghai, China) and separated by sodium dodecyl sulfate-polyacrylamide gel electrophoresis (SDS-PAGE, Beyotime, Shanghai, China), followed by electroblotting onto polyvinylidene difluoride (PVDF) membranes, which were first incubated with primary antibodies against CD9, CD63, TSG101, calnexin (all from affinity, Jiangsu, China), GAPDH (Proteintech, Chicago, USA), VEGF (Proteintech, Chicago, USA), and HIF-1α (Abcam, Cambridge, UK) at 4 °C overnight and then with horseradish peroxidase (HRP)-conjugated secondary antibody (Beyotime, Shanghai, China) at room temperature for 1h. Protein bands were detected using an enhanced chemiluminescence kit (Thermo Fisher Scientific, Waltham, MA, USA) and protein levels were analyzed using ImageJ software.

Preparation and Characterization of the PF-127 Hydrogel

The PF-127 hydrogel was synthesized as previously reported, with a few modifications.[27] Briefly, Pluronic F-127 powder (Sigma-Aldrich, St Louis, MO, USA) was slowly dissolved in PBS at 4 °C overnight, with the final concentrations of 16%, 18%, 20%, 22%, and 24% (w/v). Then, we measured gelatinization time at 26°C and 37°C of hydrogels with different concentrations using an inversion method.

HUVECs and hASCs were used to investigate the biocompatibility and cytotoxicity of the PF-127 hydrogel in vitro. First, the HUVECs or hASCs were seeded onto 48-well plates and treated with different doses of hydrogel (0, 2, 4, 6, 8,

and 10 μL). After co-culture for 2 and 4 days, cytotoxicity was evaluated as the relative viability of the cells using the CCK-8 reagent.

Subsequently, the degradation behaviors of the hydrogel and hydrogel/exosomes were assessed. Briefly, 40 μL PBS was added to 1 mL of samples (n = 4) in 1.5 mL Eppendorf tubes with and incubated at 37°C in a cell incubator. After removing the surface liquid from the hydrogels, the weight of the residual hydrogels was measured daily. The degradation rate of the PF-127 hydrogel and PF-127 hydrogel/hASC-Exos was assessed by weighing the original mass (M0) and the mass at the prescribed time points (M1) and was calculated as (M0 – M1)/M0 × 100%.[21]

Release Kinetics of PF-127 Hydrogel Encapsulated hASC-Exos

To prepare the PF-127 hydrogel loaded with exosomes, an appropriate amount of hASC -Exos was added to 18% gel in liquid state at 4°C and then solidified at 37 °C Then, the samples (n = 4) were incubated with PBS in 1.5 mL Eppendorf tubes at 37 °C in a cell incubator and were renewed at predefined times every day; the liquids were collected, and an equal volume of PBS was added. Finally, the exosomes released from the hydrogels were quantified using an Enhanced BCA protein assay kit (Beyotime, Shanghai, China) following the manufacturer's instructions, and expressed as the cumulative release percentage.

Autologous Fat Transplantation Experiments in an Animal Model

All animal experiments were approved by the Guidelines of Care and Use Committee of the First Affiliated Hospital of Wenzhou Medical University (WYYY-IACUC-AEC-2023-001) and were performed in accordance with the National Institutes of Health Guide for the Care and Use of Experimental Animals. Ten healthy specific-pathogen-free (SPF)-grade male BALB/c nude mice (6 weeks old, approximately 17−21g) were purchased from the Zhejiang Vital River Laboratory to establish the autologous fat transplantation model as described previously,[30] with a few modifications. Briefly, each mouse received a subcutaneous injection of fat (0.5 mL) at four dorsal sites. To better stimulate the migration of peripheral HUVECs and promote vascularization[31] as well as fat regeneration,[3] PBS (100 μL), PF-127 hydrogel (100 μL), hASC-Exos (5 μg/100 μL) and PF-127 hydrogel/ hASC-Exos (100 μL, containing 5 μg hASC-Exos) were carefully injected into four different peripheral regions of the grafts in each group. The mice were housed in an SPF laboratory. At 4 and 8 weeks post-implantation, the mice were sacrificed using CO_2 inhalation, and the grafts were harvested for subsequent experiments.

Histology and Immunofluorescence (IF) Staining

At the indicated time points, grafts were carefully harvested, fixed in 4% paraformaldehyde (PFA) overnight, and embedded in paraffin after dehydration. The embedded samples were cut into 5-μm thick sections which were stained with hematoxylin and eosin (HE) and Masson's trichrome (MT) to estimate the pathological changes and the degree of fibrosis in the transplanted tissue.[32] Furthermore, to analyze the vessels regeneration within the grafts and the underlying mechanism, immunofluorescent (IF) staining for CD31 (affinity, Jiangsu, China), α-SMA (affinity, Jiangsu, China), and immunochemical (IHC) analysis including HIF-1α (Abcam, Cambridge, UK), VEGF (Proteintech, Chicago, USA) were performed according to the manufacturer's instructions. Images were acquired, and the positive expression levels of the markers mentioned above were measured using the ImageJ software.

Statistical Analysis

The experimental results were analyzed using Graph Pad Prism (Version 9.0) and expressed as means ± standard deviation (SD). Differences between two groups were analyzed using unpaired Student's *t*-test, and differences between more than two groups were analyzed using one-way analysis of variance (ANOVA). Statistical significance was set at $P < 0.05$.

Results

Identification of hASCs

P3 hASCs morphology, observed under a light microscope, revealed a typical spindle-like shape (Figure 1A). Next, the trilineage differentiation potential of the hASCs was evaluated using adipogenesis, osteogenesis, and chondrogenesis assays (Figure 1B). We measured the representative surface markers of hASCs, such as CD29, CD31, CD44, CD45, and

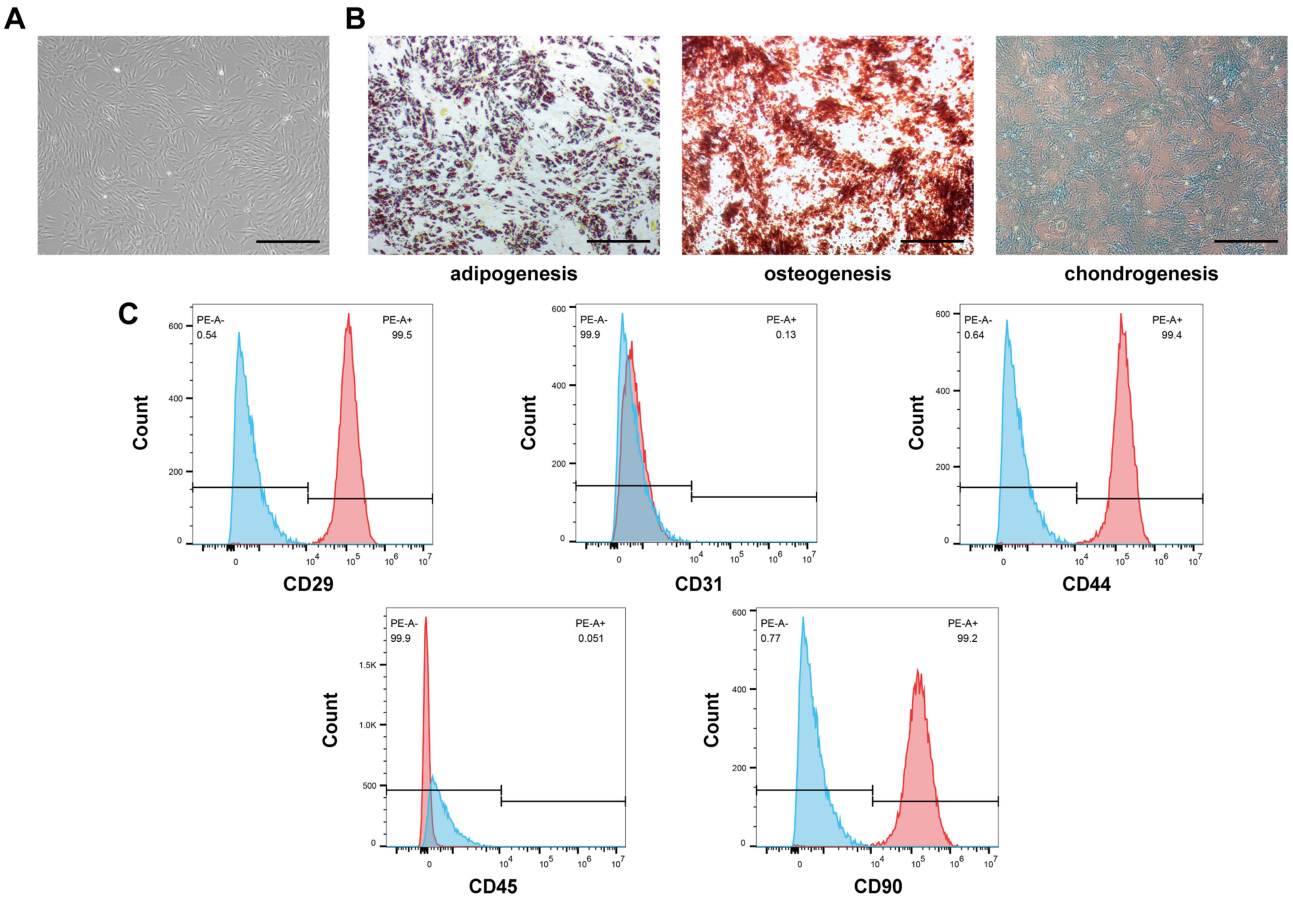

Figure 1 Identification of hASCs. (**A**) Representative image showing the typical spindle-like shape of hASCs under a light microscope. Scale bar: 500 μm. (**B**) Oil Red O, Alizarin Red, and Alcian Blue were used to detect the adipogenic, osteogenic, and chondrogenic differentiation of hASCs. Scale bar: 500 μm. (**C**) Characteristic surface markers of hASCs evaluated by flow cytometry analysis. The cells were remarkably positive for CD29, CD44 and CD90, but negative for CD31, or CD45.

CD90, using flow cytometry. The results showed that the cells were highly positive for CD29, CD44, and CD90 but negative for CD31 and CD45 (Figure 1C), consistent with the properties of stem cells. Taken together, these findings confirmed the success of hASCs isolation.

Characterization of hASC-Exos

As shown in Figure 2A, isolated hASC-Exos were observed using TEM, which revealed the presence of a typical saucer-cup morphology with a double membrane. NTA was used to measure the size distribution of hASC-Exos (Figure 2B), and the majority of these microparticles were approximately 137.2 nm. Western blotting detected exosome-specific markers (CD9, TSG101, and CD63) in hADSC-Exos, whereas calnexin was expressed only in hADSCs (Figure 2C). Collectively, these results indicated that we successfully extracted hASC-Exos.

Pro-Angiogenic Effects of hASC-Exos on HUVECs

To further evaluate the role of hASC-Exos in HUVECs, Dil-labeled hASC-Exos were co-cultured with HUVECs for 24 h. As shown in Figure 3A, a large amount of Dil-labeled Exos (red fluorescence) was taken up by the HUVECs and distributed around the nuclei (blue fluorescence).

Next, we assessed cell proliferation, migration, and tubule formation, which are key factors in angiogenesis, to examine whether hASC-Exos regulate the viability of HUVECs. As shown in Figure 3B, the CCK-8 results demonstrated that hASC-Exos stimulation significantly promoted cell proliferation on days 1, 3, and 5 compared to the control group. The migratory ability of the HUVECs was examined using scratch healing (Figure 3C) and transwell assays (Figure 3D).

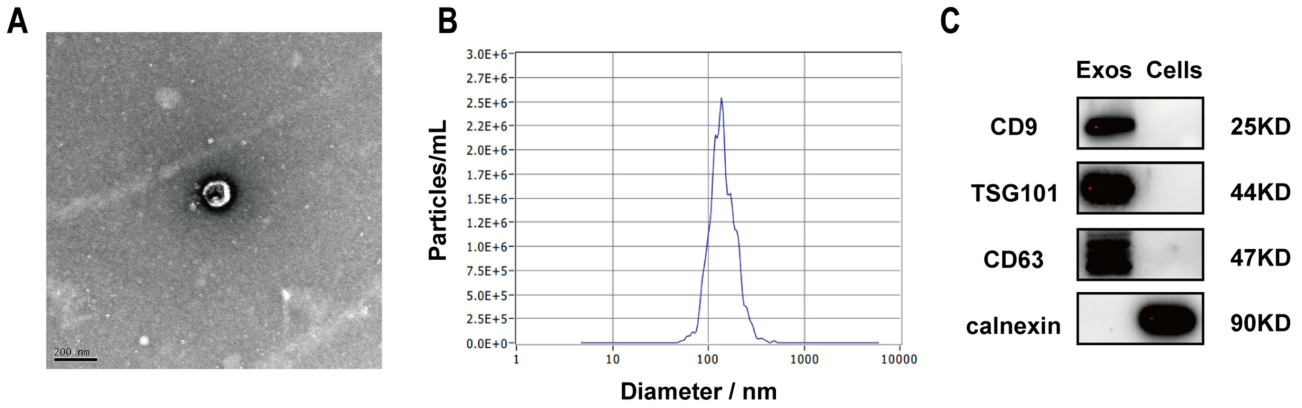

Figure 2 Characterization of isolated hASC-Exos. (**A**) Representative image of hASC-Exos morphology obtained using transmission electron microscopy (TEM). Scale bar: 200 nm. (**B**) Particle size distribution of hASC-Exos measured using nanoparticle tracking analysis (NTA). (**C**) Western blotting analysis of CD9, TSG101, CD63, and calnexin protein expression in hASC-Exos and hASCs.

The wound closure ratio (Figure 3E) and the number of migrated cells (Figure 3F) treated with hASC-Exos were significantly increased compared to those in the control group, indicating that HUVECs stimulated with 50 μg/mL hASC-Exos possessed remarkable mobility and migratory capacity. Additionally, we evaluated the effect of hASC-Exos on the tube formation capacity of HUVECs in vitro. As shown in Figure 3G and H, more total meshes, branch points, and tubes were formed when HUVECs were stimulated with hASC-Exos than in the PBS-treated group. Taken together, these observations indicated that hASC-Exos have excellent biological activity in HUVECs.

To determine the underlying molecular mechanisms in HUVECs regulated by hASC-Exos, we verified the HIF-1α/VEGF signaling pathway via Western blot analyses. As shown in Figure 3I and J, the protein expression level of HIF-1α and VEGF were significantly upregulated compared to the PBS-treated group, which indicated that the HIF-1α/VEGF signaling pathway may be activated in the vascularization of hASC-Exos.

Characterization of the PF-127 Hydrogel

Injectable thermosensitive hydrogels are promising carriers for cell and exosome delivery. In this study, we successfully constructed a thermosensitive PF-127 hydrogel that was in the liquid state at 4 °C but cross-linked to gelation at 37 °C (Figure 4A). Then we combined the PF-127 hydrogel and hASC-Exos to generate PF-127 hydrogel/hASC-Exos composites with different PF-127 concentrations (18%, 20%, 22%, 24%, and 26% (w/v)) and assessed the respective gelling time at 26 °C and 37 °C (Table 1). As the concentration of PF-127 increased, the gelling time decreased gradually. Furthermore, the results indicated that the addition of exosomes did not hamper the gelation process. Only 18% PF-127 hydrogel/hASC-Exos composite was liquid at 26°C but cross-linked to gelation at 37 °C, so we selected this concentration for the subsequent experiment.

The biocompatibility of the PF-127 hydrogel is a key prerequisite for autologous fat transplantation. The results of the CCK-8 test demonstrated that after incubating hASCs/HUVECs with different doses of hydrogels for different durations, each group of cells had equal proliferative capability and cell viability (Figure 4B), demonstrating that the hydrogels possessed good biocompatibility with hASCs and HUVECs.

Moreover, PF-127 hydrogel and PF-127 hydrogel/hASC-Exos were degraded. The hydrogel group and hydrogel/exosome composites group incubated in PBS at 37 °C gradually degraded within 6 days in a similar tendency (Figure 4C), indicating that the PF-127 hydrogel degraded well in vitro and the addition of hASC-Exos did not affect the degradation process. In general, the properties of the PF-127 hydrogel, including temperature sensitivity, biocompatibility, and degradability, enable its ideal application in autologous fat transplantation.

Exosomes Release Kinetics

To confirm that the hASC-Exos were released from the PF-127 hydrogel, we performed a micro-BCA Protein Assay to evaluate the exosome release profile. The release curve showed that the hASC-Exos loaded in the PF-127 hydrogel were completely released in 6 days in vitro and half-released on the third day (Figure 4D), showing similar trends with the

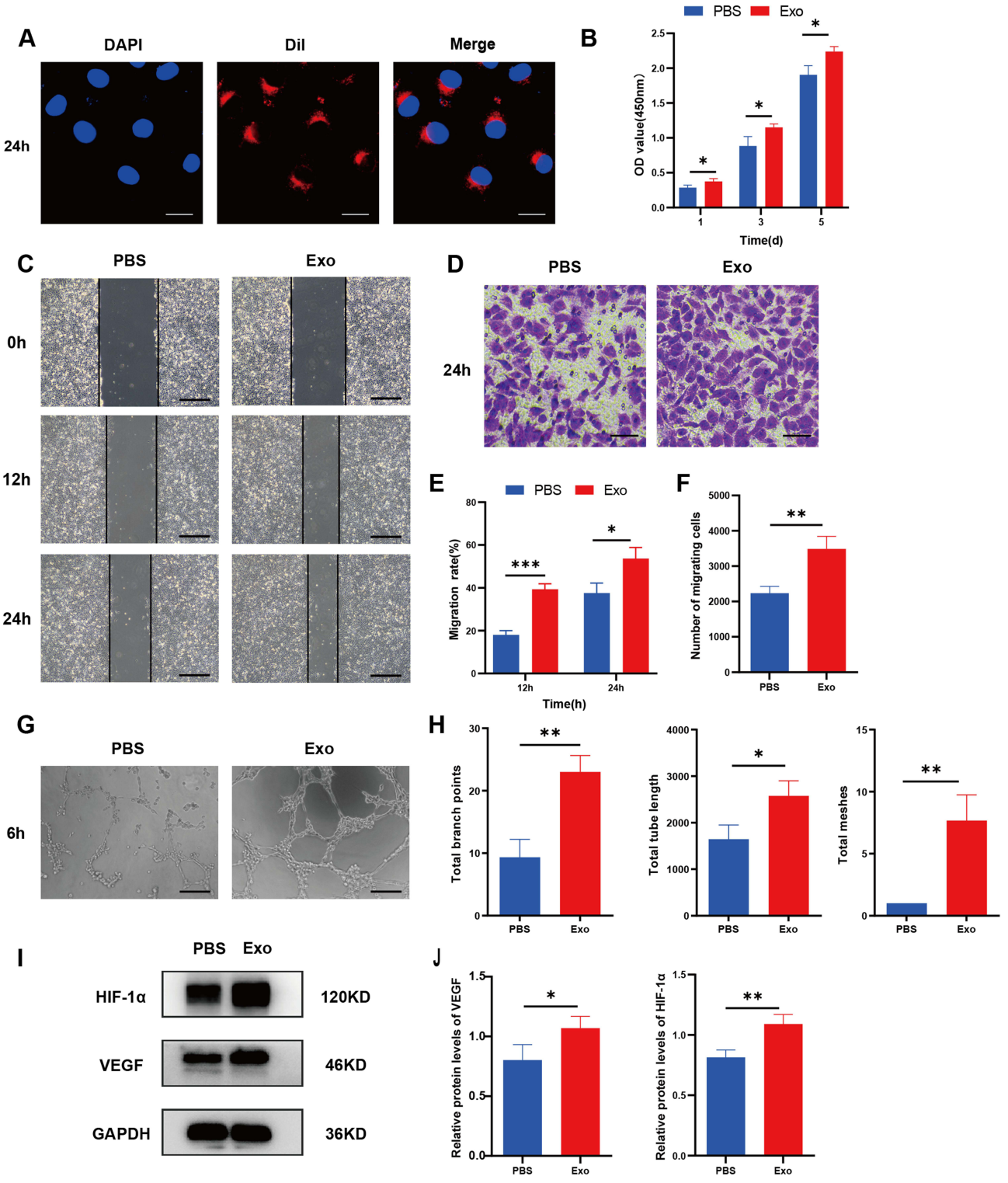

Figure 3 Internalization of hASC-Exos by HUVECs promotes their angiogenic activities. (**A**) Representative fluorescence micrograph of DiI (red)-labeled hASC-Exos internalized by HUVECs. Nuclei were stained blue with DAPI. Scale bar: 25 μm. (**B**) CCK-8 assay for proliferation of HUVECs cultured with hASC-Exos on days 1, 3, and 5. (**C**) Scratch assay of HUVECs cultured with hASC-Exos. Scale bar: 400 μm. (**D**) Transwell assay of HUVECs cultured with hASC-Exos. Scale bar: 100 μm. Quantitative analysis of (**E**) scratch assay and (**F**) transwell assay. (**G**) Tube formation assay of HUVECs cultured with hASC-Exos. Scale bar: 200 μm. (**H**) Quantitative analysis (total meshes, branch points, and tube length) of HUVECs cultured with hASC-Exos. (**I**) Western blot assay and (**J**) Quantitative analysis (HIF-1α, VEGF) for HUVECs cultured with hASCs-Exos. Data are presented as the mean ± SD of three replicates. *p < 0.05, **p < 0.01, ***p < 0.001.

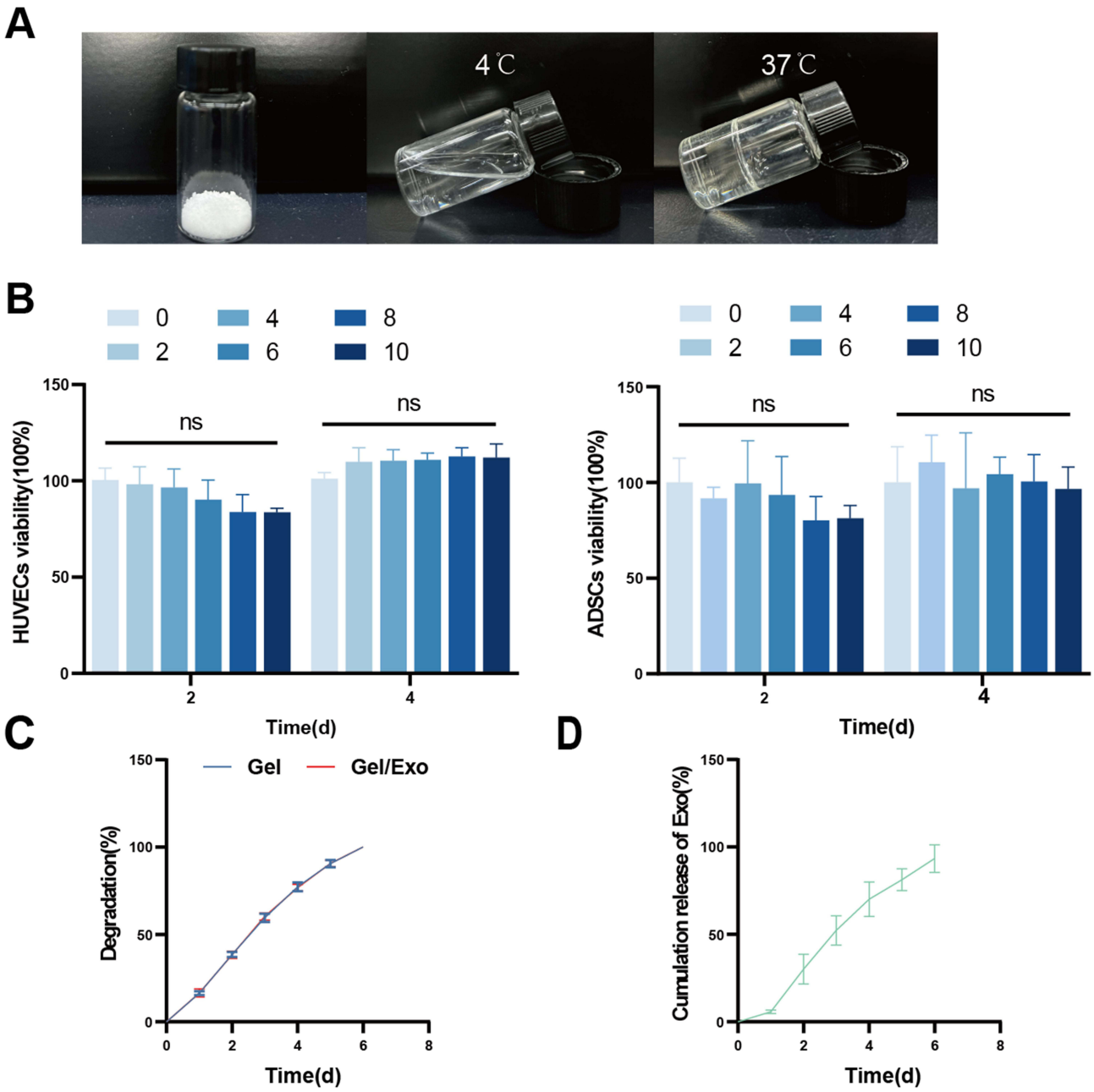

Figure 4 Characteristics of PF-127 hydrogel. (**A**) The synthesis and temperature sensitive behavior of PF-127 hydrogel. (**B**) Biocompatibility of the PF-127 hydrogel was analyzed using a CCK-8 kit. The viability of HUVECs and ASCs co-incubated with different hydrogel doses at specific time points was determined. (**C**) In vitro degradation ratio of PF-127 hydrogel and PF-127 hydrogel/hASC-Exos. (**D**) The cumulative release profile of hASC-Exos loaded into the PF-127 hydrogel was determined using an enhanced BCA protein assay kit. Data are presented as the mean ± SD of three replicates.
Abbreviation: ns, not significant.

degradation profile. More importantly, hASC-Exos were released at a steady rate over a long period, which can ensure a continuous positive biological effect on the survival of autologous fat grafts.

Fat Graft Survival Assessment

Fat was harvested and cut into pieces (Figure 5A), and each mouse received a subcutaneous injection of fat (0.5 mL) at four dorsal sites (Figure 5B). Subsequently, PBS, PF-127 hydrogel, hASC-Exo, and PF-127 hydrogel/Exo were carefully injected into four different peripheral regions of the grafts in each group (Figure 5C). The grafts were harvested at 4 and 8 weeks after transplantation. As shown in Figure 5D, the PF-127 hydrogel/hASC-Exo group had larger graft sizes and

Table 1 Gelling Time of PF-127/hASC-Exos Composites with Different PF-127 Concentrations

PF-127 Concentration (%)	Gelling Time at 26 °C	Gelling Time at 37 °C
16	No-gel	No-gel
18	No-gel	4min53s±12s
20	11min54s±5s	1min54s±5s
22	3min7s±6s	1min6s±5s
24	1min54s±5s	45s±4s

more new capillaries than the other three groups. The volume (Figure 5E) in the PF-127 hydrogel/hASC-Exos group were higher than those in the control ($p < 0.0001$) and pure hASC-Exos groups ($p < 0.001$) after 4 and 8 weeks of treatment. In addition, the weights (Figure 5F) in the PF-127 hydrogel/hASC-Exos group were also higher than in the control ($p < 0.01$ and $p < 0.0001$, respectively), and pure hASC-Exo groups ($p < 0.05$ and $p < 0.0001$, respectively) after 4 and 8 weeks, indicating that the PF-127 hydrogel/hASC-Exos positively influenced the survival of fat grafts. The mean sample volumes were 0.37 ± 0.02, 0.38 ± 0.02, 0.40 ± 0.02, 0.47 ± 0.02 (mL) (4 weeks), 0.11 ± 0.02, 0.12 ± 0.03, 0.30 ± 0.03, 0.42 ± 0.05 (mL) (8 weeks), and the mean weights were 0.37 ± 0.05, 0.36 ± 0.05, 0.40 ± 0.03, 0.49 ± 0.04 (g) (4 weeks), 0.08 ± 0.02, 0.09 ± 0.04, 0.28 ± 0.02, 0.39 ± 0.04 (g) (8 weeks), in the PBS, PF-127 hydrogel, hASC-Exos and PF-127 hydrogel/hASC-Exos groups, respectively.

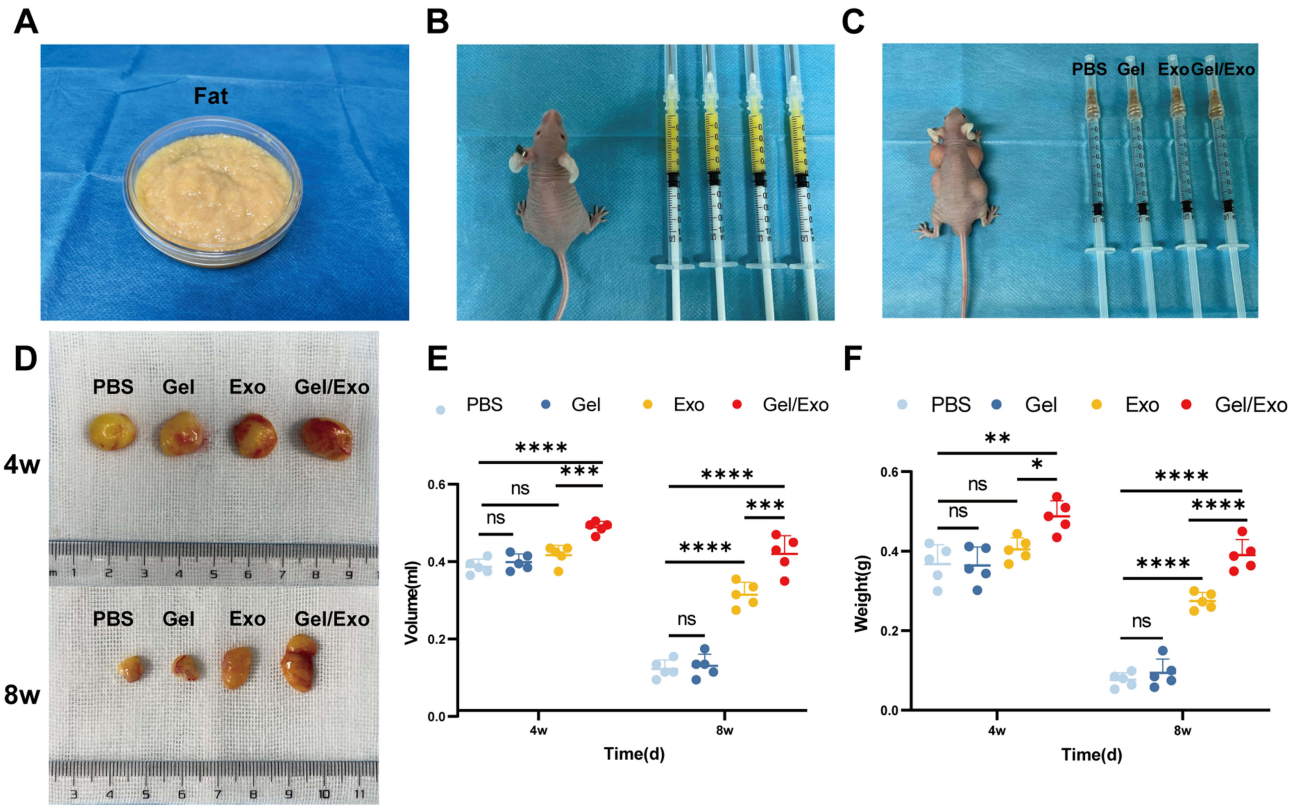

Figure 5 The process of transplantation. (**A**) Pre-cut fat. (**B**) Each nude mouse received a subcutaneous injection of fat (0.5 mL) at four dorsal sites. (**C**) PBS, PF-127 hydrogel, hASC-Exos, or PF-127 hydrogel/hASC-Exos were injected at four separate locations along the graft site in each mouse. (**D**) Representative images of the general morphology of the fat grafts after 4 and 8 weeks. (**E**) Weight of the fat grafts 4 and 8 weeks after transplantation. (**F**) Volume of the fat grafts 4 and 8 weeks after transplantation. Data are presented as the mean ± SD of five replicates. *p < 0.05, **p < 0.01, ***p < 0.001, ****p < 0.0001.
Abbreviation: ns, not significant.

Histological Evaluation

Fat graft survival after treatment with PF-127 hydrogel/hASC-Exos was further assessed using HE and MT staining. As shown in Figure 6A, cell infiltration in the PF-127 hydrogel/hASC-Exos and hASC-Exos groups was remarkably lower than that in the other groups, and the PF-127 hydrogel/hASC-Exos group was superior to the hASC-Exos group. Furthermore, the morphological integrity of fat grafts in the PF-127 hydrogel/hASC-Exos group was significantly better than that in the other groups. Moreover, MT staining results showed that cystic changes and fibrosis in the PF-127 hydrogel/ASC-Exos group were lower than those in all other groups. The control group showed the most severe fibrosis, similar to the PF-127 hydrogel alone group (Figure 6B). These results suggested that the PF-127 hydrogel-supported hASC-Exos and hASC-Exos encapsulated in the PF-127 hydrogel promoted the survival of transplanted fat.

PF-127 Hydrogel/hASC-Exos Promote Angiogenesis After Fat Transplantation

CD31 and α-SMA staining of fat sections was performed to identify new vessels. The results revealed that the expression of CD31 (Figure 7A and B) and α-SMA (Figure 7C and D) were the highest in the PF-127 hydrogel/hASC-Exo group compared to the other three groups at 8 weeks after treatment, whereas the CD31 positive cells from the hASC-Exo group were higher and the PF-127 hydrogel group was similar to that of the control group, indicating that hASC-Exos have the capacity to accelerate angiogenesis and hASC-Exos encapsulated in the PF-127 hydrogel possessed a greater pro-angiogenic effect on the fat grafts.

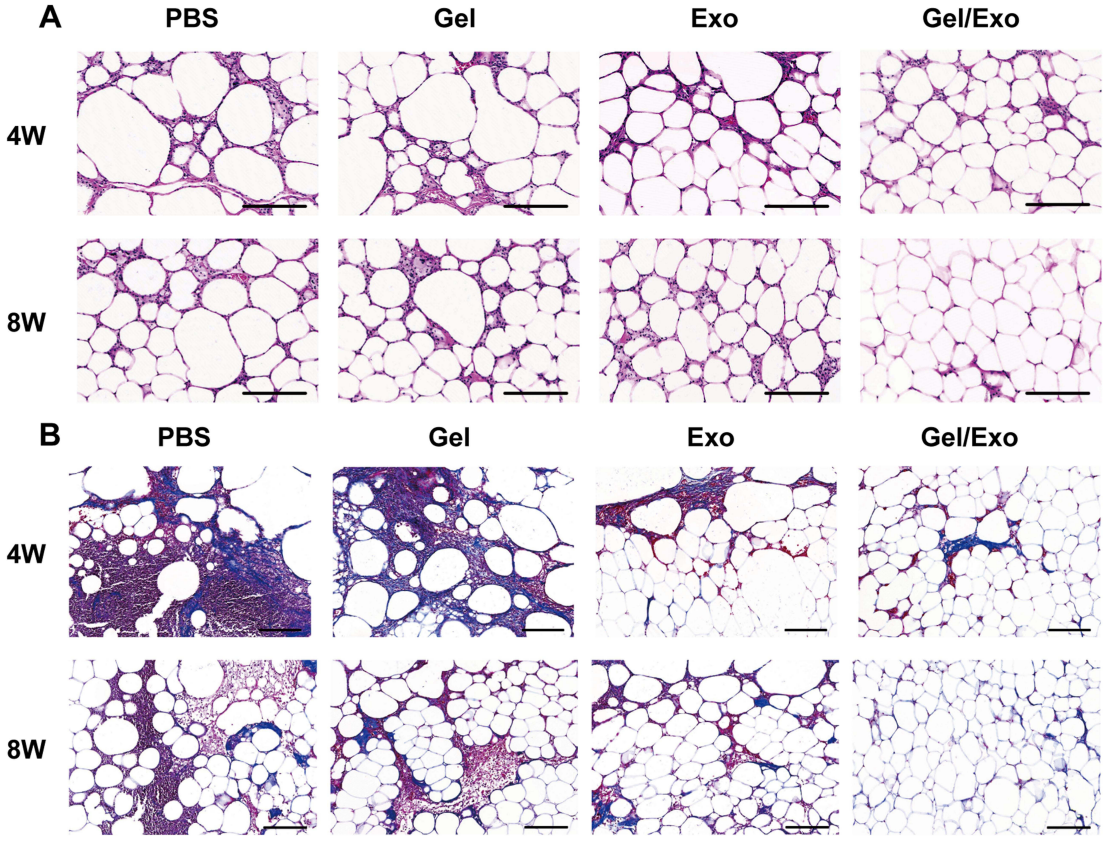

Figure 6 Histological evaluation of the harvested fat. (**A**) Representative HE-stained images of fat grafts in the different treatment groups at 4 and 8 weeks after autologous fat grafting. Scale bars: 200 μm. (**B**) Representative Masson's trichrome-stained images of graft fat in different treatment groups 4 and 8 weeks after autologous fat grafting. Scale bars: 200 μm.

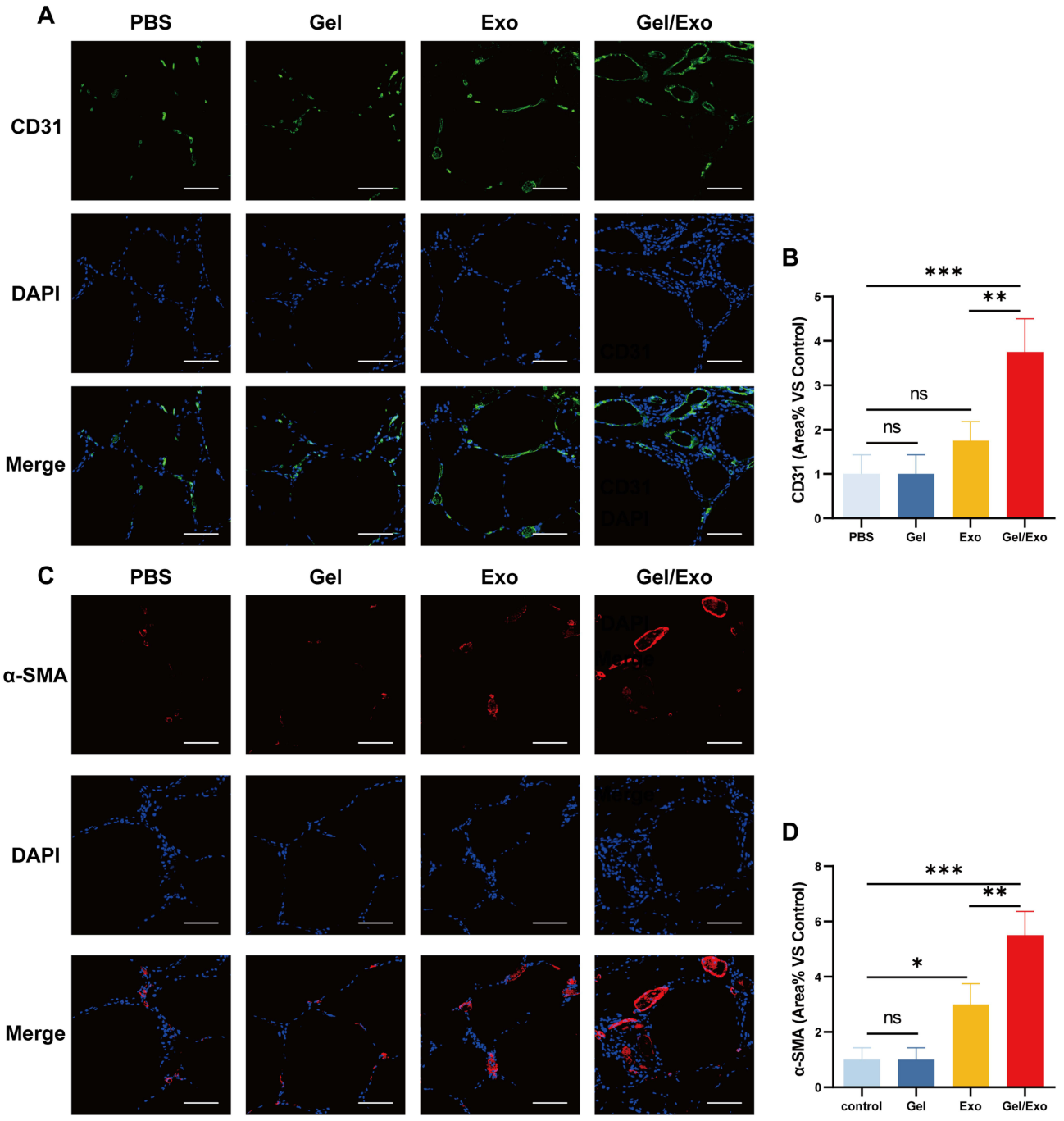

Figure 7 Neovascularization evaluation of the harvested fat treated by PF-127 hydrogel/ hASC-Exos. (**A**) Representative immunofluorescence images of CD31 (green) in fat grafts in the different treatment groups 8 weeks after autologous fat grafting. Nuclei were stained blue with DAPI. Scale bars: 100 μm. (**B**) Quantification of CD31-positive cells in the different treatment groups 8 weeks after autologous fat grafting. (**C**) Representative immunofluorescence images of α-SMA (red) in fat grafts in the different treatment groups 8 weeks after autologous fat grafting. Nuclei were stained blue with DAPI. Scale bars: 100 μm. (**D**) Quantification of SMA positive cells in the different treatment groups 8 weeks after autologous fat grafting. Data are presented as the mean ± SD of three replicates. *p < 0.05, **p < 0.01, ***p < 0.001.
Abbreviation: ns, not significant.

PF-127 Hydrogel/hASC-Exos Promote Angiogenesis by Modulating the HIF-1α/VEGF Signaling Pathway

As described above, the PF-127 hydrogel/hASC-Exos had a greater pro-angiogenic effect on fat grafts. Hence, immunohistochemical analyses of HIF-1α and VEGF were performed to further investigate their potential regulatory mechanisms. Significantly high levels of VEGF (Figure 8A and B) and HIF-1α (Figure 8C and D) were observed in the

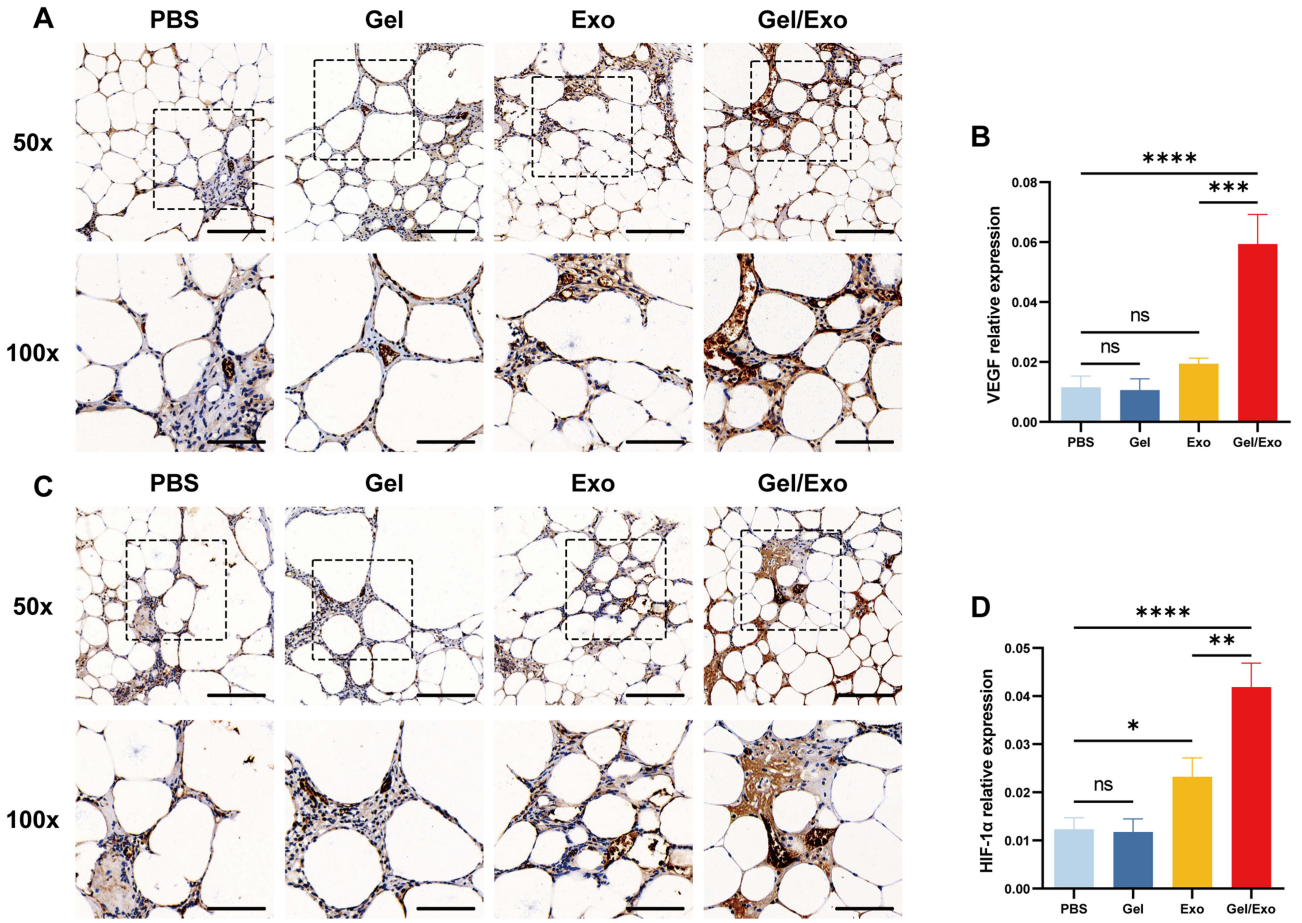

Figure 8 Histochemical analysis of VEGF and HIF-1α expression in the harvested fat. (**A**) Representative immunohistochemical staining images of VEGF at 8 weeks post-fat grafting. Scale bar: 200 μm, 100 μm. (**B**) Quantitative analysis of the relative expression of VEGF at 8 weeks post-fat grafting. (**C**) Representative immunohistochemical staining images of HIF-1α at 8 weeks post-fat grafting. Scale bar: 200 μm, 100 μm. (**D**) Quantitative analysis of the relative expression of HIF-1α at 8 weeks post-fat grafting. Data are presented as the mean ± SD of three replicates. *p < 0.05, **p < 0.01, ***p < 0.001, ****p < 0.0001.
Abbreviation: ns, not significant.

PF-127 hydrogel/hASC-Exos and hASC-Exos groups compared with those in PBS control or pure PF-127 hydrogel groups after 8 weeks of treatment, which confirmed that the activation of the HIF-1α/VEGF signal pathway by PF-127 hydrogel/hASC-Exos may facilitate new vessels formation and fat grafts survival.

Discussion

Autologous fat transplantation has been widely used in reconstructive and plastic surgery because of its abundant tissue sources, simple operation, and rapid recovery.[33] However, its low survival and high absorption rates remain major factors limiting its clinical translation and application.[34] In this study, we isolated exosomes from hASCs and found that hASC-Exos were effectively taken up by HUVECs, enhancing their proliferation, migration, and tubule formation. In addition, we fabricated a thermosensitive, biomechanical, and degradable PF-127 hydrogel to load hASC-Exos. The hASC-Exos encapsulated into the PF-127 hydrogel were injected around the fat transplant site and the hASC-Exos were slowly released and then promoted angiogenesis via activating the HIF-1α/VEGF signaling pathway, thereby improving fat grafts retention, which highlights the significance of our study.

Angiogenesis is required for the retention of fat tissue, and early rapid blood supply plays a critical role in several factors that can improve the survival of transplanted fat.[35] Although previous research has revealed that MSCs are a suitable option for use in regenerative medicine and have a positive effect on promoting angiogenesis and improving the survival of transplanted fat,[36] including hASCs,[37] an increasing number of studies have shown that the therapeutic effect of stem cells on angiogenesis

and tissue regeneration can be replaced by exosomes, which are released from stem cells and have lower immunogenicity, better stability, and storability.[38] In our study, hASCs were isolated and identified using multilineage differentiation and flow cytometry. P3 hASCs showed a typical spindle-like morphology (Figure 1A) and were positive for CD29, CD44, and CD90 but negative for CD31 and CD45 (Figure 1C). hASC-Exos were isolated by ultracentrifugation and analyzed using TEM, NTA, and Western blotting. These results indicated that we successfully extracted hASCs and hASC-Exos.

hASC-Exos are an effective strategy for promoting wound healing or treating ischemic diseases by promoting angiogenesis.[39,40] In addition, hASC-Exos have received considerable attention owing to their promising therapeutic potential for autologous fat grafting.[41] Nevertheless, the role of hASC-Exos in improving the survival of autologous fat grafts remains unclear, and the underlying molecular mechanisms require further analysis. Hence, in our in vitro study, we verified that hASC-Exos were taken up by HUVECs (Figure 3A) and significantly promoted HUVECs proliferation, migration, and tubule formation at a concentration of 50 μg/mL in comparison to the PBS control group. Western blotting was performed to determine the underlying molecular mechanisms in hASC-Exos-regulated HUVECs. Our results indicated that the HIF-1α/VEGF signaling pathway might be activated during fat vascularization, which is a new mechanism activated by hASC-Exos in autologous fat grafting.

However, because exosomes have a low retention rate in vivo, resulting in unsatisfactory treatment outcomes, we introduced a temperature-sensitive hydrogel to address this problem. Human umbilical cord-stem cell-derived exosomes encapsulated in the PF-127 hydrogel accelerated wound healing and increased the expression of VEGF and TGFβ-1 compared to the exosomes group.[23] Another recent study also confirmed that hASC-Exos encapsulated in PF-127 hydrogel promoted wound healing not only via facilitated re-epithelialization, but also by reducing inflammation.[27] These studies demonstrated that PF-127 hydrogel is a promising biomaterial carrier to deliver exosome for tissue regeneration. Therefore, in this study, we investigated whether the combined application of PF-127 hydrogels and hASC-Exos improves the survival rate of autologous fat transplantation.

Therefore, we first constructed a thermosensitive PF-127 hydrogel that was in a liquid state at 4 °C but cross-linked to gelation at 37 °C (Figure 4A). The properties of the hydrogel were identified in vitro, and our results showed that it possessed high-temperature sensitivity, biocompatibility (Figure 4B), and degradability (Figure 4C). Previous studies reported that hASCs in grafts do not die and begin to regenerate at an early stage of transplantation. It was also mentioned that the fat regeneration depended on the microenvironment especially early vascularization.[3] Our exosome release kinetics revealed that hASC-Exos were released by the PF-127 hydrogel at a steady rate over time (Figure 4D), indicating that continuous release of hASC-Exos by PF-127 hydrogel can provide a better microenvironment for fat regeneration. Taken together, these results demonstrate the efficacy and safety of the PF-127 hydrogel in the clinical translation of autologous fat grafting.

We topically applied hASC-Exos encapsulated in PF-127 hydrogel to a fat transplantation nude mouse model in vivo. As shown in Figure 5E and F, the highest weight and volume were observed in the PF-127 hydrogel/hASC-Exos group. Furthermore, we performed HE and MT staining to estimate the pathological changes and the degree of fibrosis in the fat tissue, as shown in Figure 6A and B. The PF-127 hydrogel/hASC-Exos group showed less cell infiltration, less fibrosis, and better fat cells morphology than the other groups. IF staining of CD31 (Figure 7A and B) and α-SMA (Figure 7C and D) also showed that hASC-Exos facilitated angiogenesis and that the PF-127 hydrogel loaded with hASC-Exos exerted a greater pro-angiogenic effect on fat transplantation. Vascularization involves multiple molecular pathways. Previous studies have shown that exosomes from hypoxia-treated human ASCs facilitated angiogenesis by regulating the VEGF/VEGF-R signaling pathway.[42] Additionally, hASC-Exos embedded hydrogels accelerated diabetic wound healing via the activation of miR-144-3p/NFE2L2/HIF1α signaling.[39] In our study, IHC results showed that the expression of HIF-1α and VEGF was regulated in the hASC-Exo group and was highest in the PF-127 hydrogel/hASC-Exos group (Figure 8), suggesting that activation of the HIF-1α/VEGF signaling pathway by PF-127 hydrogel/hASC-Exos may facilitate new vessel formation and improve the survival rate of transplantation fat.

Our study successfully demonstrated that the PF-127 hydrogel loaded with hASC-Exos was efficacious in improving the survival of fat grafts. Nevertheless, there are still some limitations to our present work. First, we demonstrated that the hydrogels exhibited good in vitro degradation. Nevertheless, it is necessary to further explore the catabolism of PF-127 hydrogels in fat grafts for successful clinical applications in the future. Second, although we confirmed that exosomes were taken up by HUVECs in vitro and promoted angiogenesis of transplanted fat in vivo, the absorption and distribution of exosomes in vivo and their metabolism in various organs through immunofluorescence tracking

experiments would also be interesting to further explore. Thirdly, previous studies have demonstrated that miRNAs play a significant role in mediating vascularization effects of exosomes,[43,44] therefore, further experiments such as Western blot analysis and real-time quantitative polymerase chain reaction should be performed to elucidate which miRNAs derived from hASC-Exos activate HIF-1α/VEGF signaling in HUVECs to promote angiogenesis. Overall, whether the PF-127 hydrogel loaded with hASC-Exos can be successfully applied in humans to achieve clinical transformation still requires more basic experiments and clinical trials to further study.

Conclusion

In summary, this novel study incorporated hASC-Exos into a PF-127 hydrogel for autologous fat grafting. We demonstrated that the sustained delivery of hASC-Exos may improve the survival of autologous fat grafts by creating a regenerative microenvironment that enhances neovascularization via activating the HIF-1α/VEGF signaling pathway. Taken together, the hASC-Exos PF-127 hydrogel has significant potential for clinical translation in autologous fat transplantation.

Acknowledgments

We thank the National Natural Science Foundation of China (81971850).

Disclosure

The authors report no conflicts of interest in this work.

References

1. Niu Q, Zhang J, Lu B, et al. Oral and maxillofacial autologous fat transplantation: history, clinical application status and research progress. *Aesthetic Plast Surg*. 2022;46(1):297–307. doi:10.1007/s00266-021-02238-y
2. Li L, Pan S, Ni B, Lin Y. Improvement in autologous human fat transplant survival with SVF plus VEGF-PLA nano-sustained release microspheres. *Cell Biol Int*. 2014;38(8):962–970. doi:10.1002/cbin.10284
3. Eto H, Kato H, Suga H, et al. The fate of adipocytes after nonvascularized fat grafting: evidence of early death and replacement of adipocytes. *Plast Reconstr Surg*. 2012;129(5):1081–1092. doi:10.1097/PRS.0b013e31824a2b19
4. Geeroms M, Fujimura S, Aiba E, et al. Quality and quantity-cultured human mononuclear cells improve human fat graft vascularization and survival in an in vivo murine experimental model. *Plast Reconstr Surg*. 2021;147(2):373–385. doi:10.1097/PRS.0000000000007580
5. Mashiko T, Yoshimura K. How does fat survive and remodel after grafting? *Clin Plast Surg*. 2015;42(2):181–190. doi:10.1016/j.cps.2014.12.008
6. Li M, Ke QF, Tao SC, Guo SC, Rui BY, Guo YP. Fabrication of hydroxyapatite/chitosan composite hydrogels loaded with exosomes derived from miR-126-3p overexpressed synovial mesenchymal stem cells for diabetic chronic wound healing. *J Mater Chem B*. 2016;4(42):6830–6841. doi:10.1039/C6TB01560C
7. Wu KH, Zhou B, Lu SH, et al. In vitro and in vivo differentiation of human umbilical cord derived stem cells into endothelial cells. *J Cell Biochem*. 2007;100(3):608–616. doi:10.1002/jcb.21078
8. Hutchings G, Janowicz K, Moncrieff L, et al. The proliferation and differentiation of adipose-derived stem cells in neovascularization and angiogenesis. *Int J Mol Sci*. 2020;21(11):3790. doi:10.3390/ijms21113790
9. Storti G, Scioli MG, Kim BS, Orlandi A, Cervelli V. Adipose-derived stem cells in bone tissue engineering: useful tools with new applications. *Stem Cells Int*. 2019;2019:3673857. doi:10.1155/2019/3673857
10. Yang S, Zhu B, Yin P, et al. Integration of human umbilical cord mesenchymal stem cells-derived exosomes with hydroxyapatite-embedded hyaluronic acid-alginate hydrogel for bone regeneration. *ACS Biomater Sci Eng*. 2020;6(3):1590–1602. doi:10.1021/acsbiomaterials.9b01363
11. Yu M, Liu W, Li J, et al. Exosomes derived from atorvastatin-pretreated MSC accelerate diabetic wound repair by enhancing angiogenesis via AKT/eNOS pathway. *Stem Cell Res Ther*. 2020;11(1):350. doi:10.1186/s13287-020-01824-2
12. Riazifar M, Mohammadi MR, Pone EJ, et al. Stem cell-derived exosomes as nanotherapeutics for autoimmune and neurodegenerative disorders. *ACS Nano*. 2019;13(6):6670–6688. doi:10.1021/acsnano.9b01004
13. Wei W, Ao Q, Wang X, et al. Mesenchymal stem cell-derived exosomes: a promising biological tool in nanomedicine. *Front Pharmacol*. 2020;11:590470. doi:10.3389/fphar.2020.590470
14. Bjørge IM, Kim SY, Mano JF, Kalionis B, Chrzanowski W. Extracellular vesicles, exosomes and shedding vesicles in regenerative medicine - a new paradigm for tissue repair. *Biomater Sci*. 2017;6(1):60–78. doi:10.1039/C7BM00479F
15. Barres BA, Frühbeis C, Fröhlich D, et al. Neurotransmitter-triggered transfer of exosomes mediates oligodendrocyte–neuron communication. *PLoS Biol*. 2013;11(7). doi:10.1371/journal.pbio.1001625
16. Chang W, Wang J. Exosomes and their noncoding RNA cargo are emerging as new modulators for diabetes mellitus. *Cells*. 2019;8(8):853. doi:10.3390/cells8080853
17. Jing X, Wang S, Tang H, et al. Dynamically bioresponsive DNA hydrogel incorporated with dual-functional stem cells from apical papilla-derived exosomes promotes diabetic bone regeneration. *ACS Appl Mater Interfaces*. 2022;14(14):16082–16099. doi:10.1021/acsami.2c02278
18. Ghodrat S, Hoseini SJ, Asadpour S, Nazarnezhad S, Alizadeh Eghtedar F, Kargozar S. Stem cell-based therapies for cardiac diseases: the critical role of angiogenic exosomes. *BioFactors*. 2021;47(3):270–291. doi:10.1002/biof.1717
19. Riau AK, Ong HS, Yam GHF, Mehta JS. Sustained delivery system for stem cell-derived exosomes. *Front Pharmacol*. 2019;10:1368. doi:10.3389/fphar.2019.01368

20. Ruel-Gariépy E, Leroux J-C. In situ-forming hydrogels—review of temperature-sensitive systems. *Eur J Pharm Biopharm*. 2004;58(2):409–426. doi:10.1016/j.ejpb.2004.03.019
21. Zhang Y, Xie Y, Hao Z, et al. Umbilical mesenchymal stem cell-derived exosome-encapsulated hydrogels accelerate bone repair by enhancing angiogenesis. *ACS Appl Mater Interfaces*. 2021;13(16):18472–18487. doi:10.1021/acsami.0c22671
22. Wang C, Wang M, Xu T, et al. Engineering bioactive self-healing antibacterial exosomes hydrogel for promoting chronic diabetic wound healing and complete skin regeneration. *Theranostics*. 2019;9(1):65–76. doi:10.7150/thno.29766
23. Yang J, Chen Z, Pan D, Li H, Shen J. Umbilical cord-derived mesenchymal stem cell-derived exosomes combined pluronic F127 hydrogel promote chronic diabetic wound healing and complete skin regeneration. *Int J Nanomedicine*. 2020;15:5911–5926. doi:10.2147/IJN.S249129
24. Carvalho GC, Araujo VHS, Fonseca-Santos B, et al. Highlights in poloxamer-based drug delivery systems as strategy at local application for vaginal infections. *Int J Pharm*. 2021;602:120635. doi:10.1016/j.ijpharm.2021.120635
25. Catapano A, Akash MSH, Rehman K, Sun H, Chen S. Sustained delivery of IL-1Ra from PF127-gel reduces hyperglycemia in diabetic GK-rats. *PLoS One*. 2013;8(2):e55925.
26. Ji Z, Cai Z, Gu S, et al. Exosomes derived from human adipose-derived stem cells inhibit lipogenesis involving hedgehog signaling pathway. *Front Bioeng Biotechnol*. 2021;9:734810. doi:10.3389/fbioe.2021.734810
27. Zhou Y, Zhang XL, Lu ST, et al. Human adipose-derived mesenchymal stem cells-derived exosomes encapsulated in pluronic F127 hydrogel promote wound healing and regeneration. *Stem Cell Res Ther*. 2022;13(1):407. doi:10.1186/s13287-022-02980-3
28. Guan P, Liu C, Xie D, et al. Exosome-loaded extracellular matrix-mimic hydrogel with anti-inflammatory property Facilitates/promotes growth plate injury repair. *Bioact Mater*. 2022;10:145–158.
29. Cao Y, Xu Y, Chen C, Xie H, Lu H, Hu J. Local delivery of USC-derived exosomes harboring ANGPTL3 enhances spinal cord functional recovery after injury by promoting angiogenesis. *Stem Cell Res Ther*. 2021;12(1):20. doi:10.1186/s13287-020-02078-8
30. He Y, Yu X, Chen Z, Li L. Stromal vascular fraction cells plus sustained release VEGF/Ang-1-PLGA microspheres improve fat graft survival in mice. *J Cell Physiol*. 2019;234(5):6136–6146. doi:10.1002/jcp.27368
31. Yang K, Li D, Wang M, et al. Exposure to blue light stimulates the proangiogenic capability of exosomes derived from human umbilical cord mesenchymal stem cells. *Stem Cell Res Ther*. 2019;10(1):358. doi:10.1186/s13287-019-1472-x
32. Lu F, Li J, Gao J, et al. Improvement of the survival of human autologous fat transplantation by using VEGF-transfected adipose-derived stem cells. *Plast Reconstr Surg*. 2009;124(5):1437–1446. doi:10.1097/PRS.0b013e3181babbb6
33. Locke MB, de Chalain TM. Current practice in autologous fat transplantation: suggested clinical guidelines based on a review of recent literature. *Ann Plast Surg*. 2008;60(1):98–102. doi:10.1097/SAP.0b013e318038f74c
34. Anghelina M, Krishnan P, Moldovan L, Moldovan NI. Monocytes/macrophages cooperate with progenitor cells during neovascularization and tissue repair: conversion of cell columns into fibrovascular bundles. *Am J Pathol*. 2006;168(2):529–541. doi:10.2353/ajpath.2006.050255
35. Kato H, Mineda K, Eto H, et al. Degeneration, regeneration, and cicatrization after fat grafting: dynamic total tissue remodeling during the first 3 months. *Plast Reconstr Surg*. 2014;133(3):303e–313e. doi:10.1097/PRS.0000000000000066
36. Borkar R, Wang X, Zheng D, et al. Human ESC-derived MSCs enhance fat engraftment by promoting adipocyte reaggregation, secreting CCL2 and mobilizing macrophages. *Biomaterials*. 2021;272:120756. doi:10.1016/j.biomaterials.2021.120756
37. Zhao H, Shang Q, Pan Z, et al. Exosomes from adipose-derived stem cells attenuate adipose inflammation and obesity through polarizing M2 macrophages and beiging in white adipose tissue. *Diabetes*. 2018;67(2):235–247. doi:10.2337/db17-0356
38. Wang M, Wang C, Chen M, et al. Efficient angiogenesis-based diabetic wound healing/skin reconstruction through bioactive antibacterial adhesive ultraviolet shielding nanodressing with exosome release. *ACS Nano*. 2019;13(9):10279–10293. doi:10.1021/acsnano.9b03656
39. Hu N, Cai Z, Jiang X, et al. Hypoxia-pretreated ADSC-derived exosome-embedded hydrogels promote angiogenesis and accelerate diabetic wound healing. *Acta Biomater*. 2023;157:175–186. doi:10.1016/j.actbio.2022.11.057
40. Shiekh PA, Singh A, Kumar A. Exosome laden oxygen releasing antioxidant and antibacterial cryogel wound dressing OxOBand alleviate diabetic and infectious wound healing. *Biomaterials*. 2020;249:120020. doi:10.1016/j.biomaterials.2020.120020
41. Zhang Y, Liu T. Adipose-derived stem cells exosome and its potential applications in autologous fat grafting. *J Plast Reconstr Aesthet Surg*. 2023;76:219–229. doi:10.1016/j.bjps.2022.10.050
42. Han Y, Ren J, Bai Y, Pei X, Han Y. Exosomes from hypoxia-treated human adipose-derived mesenchymal stem cells enhance angiogenesis through VEGF/VEGF-R. *Int J Biochem Cell Biol*. 2019;109:59–68. doi:10.1016/j.biocel.2019.01.017
43. Wu D, Qin H, Wang Z, et al. Bone mesenchymal stem cell-derived sEV-encapsulated thermosensitive hydrogels accelerate osteogenesis and angiogenesis by release of exosomal miR-21. *Front Bioeng Biotechnol*. 2021;9:829136. doi:10.3389/fbioe.2021.829136
44. Qu Q, Liu L, Cui Y, et al. miR-126-3p containing exosomes derived from human umbilical cord mesenchymal stem cells promote angiogenesis and attenuate ovarian granulosa cell apoptosis in a preclinical rat model of premature ovarian failure. *Stem Cell Res Ther*. 2022;13(1):352. doi:10.1186/s13287-022-03056-y